

# Unusual Electronic Structure and Observation of Dispersion Kink in CeFeAsO Parent Compound of FeAs-Based Superconductors

Haiyun Liu<sup>1</sup>, G. F. Chen<sup>2</sup>, Wentao Zhang<sup>1</sup>, Lin Zhao<sup>1</sup>, Guodong Liu<sup>1</sup>, T.-L. Xia<sup>2</sup>, Xiaowen Jia<sup>1</sup>, Daixiang Mu<sup>1</sup>, Shanyu Liu<sup>1</sup>, Shaolong He<sup>1</sup>, Yingying Peng<sup>1</sup>, Junfeng He<sup>1</sup>, Zhaoyu Chen<sup>1</sup>, Xiaoli Dong<sup>1</sup>, Jun Zhang<sup>1</sup>, Guiling Wang<sup>3</sup>, Yong Zhu<sup>3</sup>, Zuyan Xu<sup>3</sup>, Chuangtian Chen<sup>3</sup> and X. J. Zhou<sup>1,\*</sup>

<sup>1</sup>National Lab for Superconductivity, Beijing National Laboratory for Condensed Matter Physics, Institute of Physics, Chinese Academy of Sciences, Beijing 100190, China

<sup>2</sup>Department of Physics, Renmin University of China, Beijing 100872, China

<sup>3</sup>Technical Institute of Physics and Chemistry, Chinese Academy of Sciences, Beijing 100190, China

(Dated: December 15, 2009)

We report the first comprehensive high-resolution angle-resolved photoemission measurements on CeFeAsO, a parent compound of FeAs-based high temperature superconductors with a magnetic/structural transition at  $\sim 150$  K. In the magnetic ordering state, four hole-like Fermi surface sheets are observed near  $\Gamma(0,0)$  and the Fermi surface near  $M(\pm\pi, \pm\pi)$  shows a tiny electron-like pocket at M surrounded by four strong spots. The unusual Fermi surface topology deviates strongly from the band structure calculations. The electronic signature of the magnetic/structural transition shows up in the dramatic change of the quasiparticle scattering rate. A dispersion kink at  $\sim 25$  meV is for the first time observed in the parent compound of Fe-based superconductors.

PACS numbers: 74.70.-b, 74.25.Jb, 79.60.-i, 71.20.-b

The recent discovery of Fe-based superconductors[1–5] has attracted much attention because it represents the second class of high- $T_c$  superconductors after the first discovery of high- $T_c$  copper-oxide superconductors. The parent compound is antiferromagnetic[6, 7]; superconductivity is realized by suppressing the magnetic ordering through chemical doping[1–5] or applying high pressure[8]. Understanding the nature and origin of the magnetic ordering is thus crucial in understanding the interplay between magnetism and superconductivity in the Fe-based superconductors. Among various Fe-based families[1–5], the LnFeAsO system (so-called 1111-type with Ln representing rare earth elements) is particularly interesting because of its highest  $T_c$  ( $\sim 55$  K)[2] which remains the only family with  $T_c$  above 40 K so far. Despite being the first Fe-based superconductors discovered[1], the 1111-type compounds have not been studied extensively due to the difficulty in obtaining high quality and sizable single crystal samples. While a number of angle-resolved photoemission (ARPES) measurements have been performed on the (Ba,Sr)Fe<sub>2</sub>As<sub>2</sub> parent compounds (so-called 122-type)[9–15], very few detailed ARPES studies have been carried out on the FeAs-based 1111-type compounds[16, 17]. Investigation of the 1111 family is important not only to understand its unique high  $T_c$  but also to sort out universal features among various families that are generic for high- $T_c$  superconductivity in the Fe-based superconductors.

In this paper we report first comprehensive high resolution ARPES measurement on CeFeAsO. Unusual Fermi surface topology in the magnetic ordering state is observed: (1). Four hole-like Fermi surface sheets are observed near  $\Gamma(0,0)$  that are different from three sheets expected from band structure calculations; (2). The

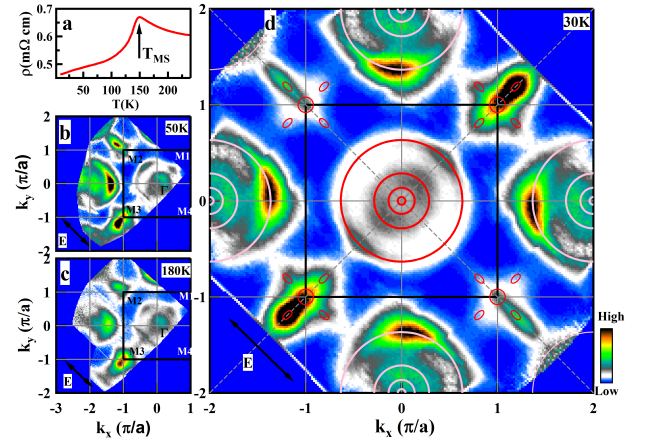


FIG. 1: (a). Resistivity–temperature dependence of CeFeAsO single crystal. (b). Spectral intensity as a function of  $k_x$  and  $k_y$  integrated over a  $[-5$  meV,  $5$  meV] energy window with respect to the Fermi level at 50 K. (c). Fermi surface mapping at 180 K on the same sample as (b). The incident light polarization is marked as the black arrows. (d). Fermi surface mapping at 30 K from another CeFeAsO sample.

Fermi surface near  $M(\pm\pi, \pm\pi)$  is composed of a tiny electron-like Fermi pocket at M surrounded by four strong spots that is dramatically different from large electron-like Fermi surfaces expected from band structure calculations. The electronic signature of the magnetic/structural transition shows up in CeFeAsO in the obvious change of the quasiparticle scattering rate. For the first time we have observed the development and enhancement of dispersion kink at  $\sim 25$  meV in the magnetically-ordered state. These results will shed key light on understanding the magnetism and superconductivity in the

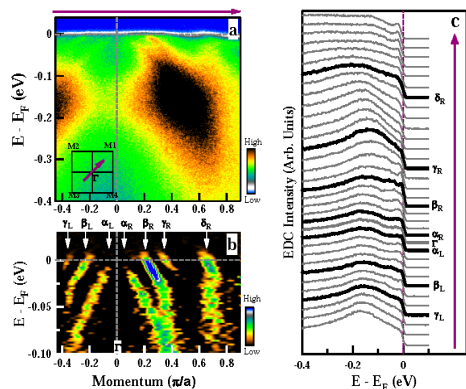


FIG. 2: Electronic structure of CeFeAsO near  $\Gamma$  measured at 20 K. (a). Original photoemission image measured on a  $\Gamma$ -M cut as shown in the inset. (b). Second derivative image obtained from (a) with all Fermi crossings marked. (c). Corresponding EDCs with those at  $k_F$  marked as thick lines.

Fe-based superconductors.

The ARPES measurements were carried out using our lab system equipped with Scienta R4000 analyzer and VUV5000 UV source which gives a photon energy of Helium I at  $h\nu = 21.218$  eV[18]. The overall energy resolution is 10 meV and the angular resolution is  $\sim 0.3$  degree. The CeFeAsO single crystals with a size of  $1\sim 2$  mm were grown using flux method. The resistivity-temperature dependence is nearly identical to that of the polycrystalline CeFeAsO sample[19] with a magnetic/structural transition temperature ( $T_{MS}$ ) at  $\sim 150$  K (Fig. 1a). The crystals were cleaved *in situ* and measured in vacuum with a base pressure better than  $5 \times 10^{-11}$  Torr.

Figure 1 shows the Fermi surface mapping of CeFeAsO covering a multiple Brillouin Zones (BZs). Figs. 1b and c are original Fermi surface data measured below and above  $T_{MS} \sim 150$  K, respectively, while Fig. 1d is obtained by symmetrizing the original data under four-fold symmetry measured on another sample. The spectral intensity in the 2nd BZ is stronger than that of the first one. Also the overall spectral distribution lacks strict four-fold symmetry around  $\Gamma(0,0)$  which may be caused by the photoemission matrix-element effect. Detailed analysis of the electronic structure near  $\Gamma$ ,  $M3(-\pi, -\pi)$ , and  $M2(-\pi, \pi)$  are shown in Fig. 2, Fig. 3 and Fig. 4, respectively (we denote the four M points as M1, M2, M3 and M4, as shown in Figs. 1b and c).

The Fermi surface of CeFeAsO consists of four hole-like sheets near  $\Gamma$  in the magnetic-ordering state (Fig. 1d). This can be seen clearly from the band structure measurement along the  $\Gamma$ -M cut (Fig. 2a and 2b) where four hole-like bands are identified (denoted as  $\alpha$ ,  $\beta$ ,  $\gamma$ , and  $\delta$  in Fig. 2b). The corresponding photoemission spectra (energy distribution curves, EDCs, Fig. 2c) indicate that these four bands all cross the Fermi level with the Fermi momenta ( $k_F$ ) of 0.04 ( $\alpha$ ), 0.22( $\beta$ ), 0.35 ( $\gamma$ ), and 0.66 ( $\delta$ ) in a unit of  $\pi/a$  (lattice constant  $a=3.996$  Å). The Fermi

surface volume calculation gives an electron counting of 2 ( $\alpha$ ), 1.9 ( $\beta$ ), 1.8 ( $\gamma$ ) and 1.39 ( $\delta$ ). The Fermi velocities of these four bands are 0.34( $\alpha$ ), 0.30( $\beta$ ), 0.23( $\gamma$ ) and 0.46 ( $\delta$ ) in a unit of  $\text{eV}\cdot\text{\AA}$ . In addition to these four bands, there is also a flat band at  $\sim -0.18$  eV as seen from the EDCs in Fig. 2c.

The observation of four hole-like Fermi surface sheets near  $\Gamma$  is surprising because only three bands are expected from band structure calculations either in non-magnetic state[20] or magnetic state[21]. This is different from the previous measurement on LaFeAsO where three bands are resolved near  $\Gamma$  with only two of them crossing the Fermi level[17]. It is also different from the 122-type parent compound  $\text{BaFe}_2\text{As}_2$  where only three bands near  $\Gamma$  are observed below  $T_{MS}$ [14]. However, we note that the inner three bands of CeFeAsO ( $\alpha$ ,  $\beta$  and  $\gamma$ ) show strong resemblance to those in  $\text{BaFe}_2\text{As}_2$  [14] with even similar Fermi momenta and the outer large Fermi surface ( $\delta$ ) is similar to that observed in LaFeAsO[17] and LaFePO[22]. One immediate possibility is whether the extra band(s) in CeFeAsO is due to band folding associated with the magnetic/structural transition. We believe this is unlikely because the folding effect in CeFeAsO is weak since there is no similar hole-like bands observed near M, as we will see later in Fig. 3 and Fig. 4. In particular, the large  $\delta$  band can not be due to such a folding effect because it is present both below and above  $T_{MS}$  (Figs. 1b and c). The other possibility is whether the extra band is specific for CeFeAsO because of its Ce 4f electrons. We performed band structure calculations and found that for CeFeAsO there appear two extra large hole-like Fermi surface sheets near  $\Gamma$  from the Ce-related electronic states. The fact that we see only one ( $\delta$ ) and its strong similarity to that in LaFeAsO[17] and even LaFePO[22] makes us believe it is more likely a generic feature for the 1111-type compounds. The third possibility is whether the extra band(s) could be due to surface state. Considering the inner three bands are similar in CeFeAsO and  $\text{BaFe}_2\text{As}_2$  systems, it comes to whether the large Fermi surface  $\delta$  could be surface state common in 1111-type compounds. We note that a simple electron counting of the inner three Fermi surface ( $\alpha$ ,  $\beta$  and  $\gamma$ ) yields a total of 5.7 that is close to the expected value of 6, while the electron counting of all four sheets is 7 which is apparently larger than 6. This seems to suggest not all of four Fermi surface sheets are intrinsic that are representative of the bulk property.

The Fermi surface mapping of CeFeAsO near M (Fig. 1) is characterized as two line patches crossing each other at M: one patch is along the  $\Gamma$ -M direction with strong spectral weight in the second BZ, while the other weak patch perpendicular to the  $\Gamma$ -M direction. The two independent measurements near M2 and M3 give similar results (Fig. 1d). Similar cross-shaped pattern can also be seen near M in LaFeAsO[17]. To understand the formation of these line patches, we carried out de-

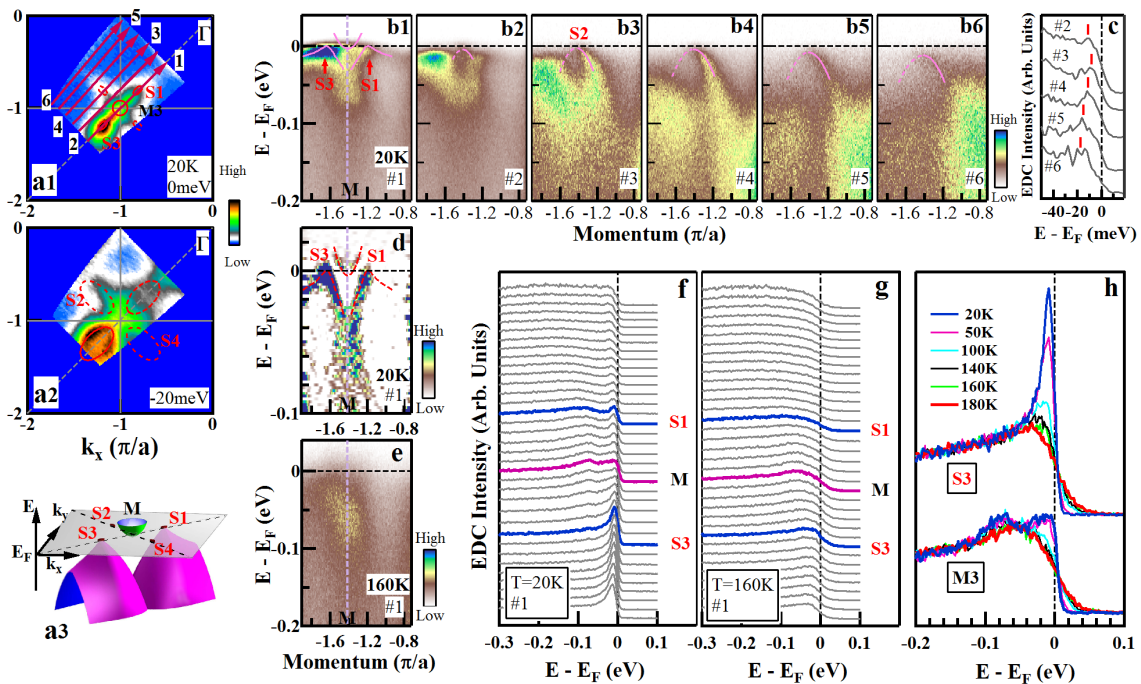


FIG. 3: Electronic structure of CeFeAsO near M3(- $\pi$ , $\pi$ ). (a). Spectral intensity as a function of  $k_x$  and  $k_y$  integrated over [-1 meV, 1 meV] (a1) and [-21 meV, -19 meV] (a2) with respect to the Fermi level measured at 20 K. The strong spot S3 in (a1) increases in area with increasing binding energy to become hole-like Fermi pocket in (a2). (a3). Schematic drawing of band structure around M. For clarity, we show only the  $\Gamma$ -M3-parallel line patch; the  $\Gamma$ -M3-perpendicular patch is similar but not drawn here. (b). Photoemission images taken along 6 typical momentum cuts with their location shown in (a1). Pink lines are guides to the eye for the band structure. (c). EDCs near the band top for cuts #2 (Fig. b2) to #6 (Fig. b6). The EDC for the cut #3 is closest to the Fermi level while the others are below the Fermi level. (d). Second derivative image from Fig. 3b1 for the cut #1. Red dashed curves denote two hole bands (S1 and S3) and an electron band at M. (e). Photoemission image of the cut #1 at 160 K. (f) and (g) show EDCs of the cut #1 at 20 K and 160 K (corresponding to Fig. 3b1 and 3e). (h). Temperature dependence of EDCs at S3 and M.

tailed momentum-dependent measurements for the  $\Gamma$ -M-parallel patch (Fig. 4b1-6 and Fig. 4c1-6) as well as for the  $\Gamma$ -M-perpendicular patch (Fig. 3b1-6). It turns out that, in both cases, the band structure along the line patch shows a series of hole-like inverse-parabolic bands; the line patch in the Fermi surface mapping then corresponds to the spectral weight from the top of these bands. The energy position of the band top shows a maximum on each side of M that is closest to the Fermi level, as seen from Fig. 3b, Fig. 4b and 4c, and more clearly from the EDCs in Fig. 3c. These give rise to four strong spots (S1, S2, S3 and S4 in Figs. 1c, 3a and 4a) around M. In addition, a careful inspection of bands right near the M point suggests the existence of a tiny electron-like pocket at M. This can be seen from the momentum cut along the  $\Gamma$ -M3 line (Fig. 3b1 and Fig. 3d for the cut #1 in Fig. 3a). Fig. 3a3 shows a schematic drawing of the band structure near M along one line patch. The peculiar Fermi surface topology near M deviates significantly from the band structure calculations which predict two crossed electron-like ellipses[20, 21]. It is also distinct from that observed in BaFe<sub>2</sub>As<sub>2</sub>[14] but bears some resemblance to

that of optimally-doped (Ba<sub>0.6</sub>K<sub>0.4</sub>)Fe<sub>2</sub>As<sub>2</sub>[12, 23, 24].

The electronic signature of magnetic/structural transition in CeFeAsO shows up in the quasiparticle scattering rate. This can be seen from the temperature evolution of the photoemission spectra at M (EDCs at M3 in Fig. 3h) and at the strong spot S3 (Fig. 3h and Fig. 4f). The EDCs at M3 (Fig. 3h) show a broad peak above  $T_{MS}$  and evolve into two-peak structure at low temperature with sharpening of the peak near the Fermi level. The change of EDCs near the strong spot S3 (Fig. 3h and Fig. 4f) is more dramatic: it evolves from a broad feature above  $T_{MS}$  into a sharp quasiparticle peak at low temperature in the magnetic ordering state. Our simulations indicate that such dramatic sharpening cannot be attributed to trivial temperature broadening in terms of Fermi distribution. Therefore, this dramatic decrease of the quasiparticle scattering rate is a clear signature of the magnetic transition.

As seen in Fig. 4, the energy bands near the strong spots (Fig. 4b4-5 near the strong spot S3) show a clear kink in the dispersion. Quantitative MDC (momentum distribution curve) analysis (Fig. 4g) indicates that the

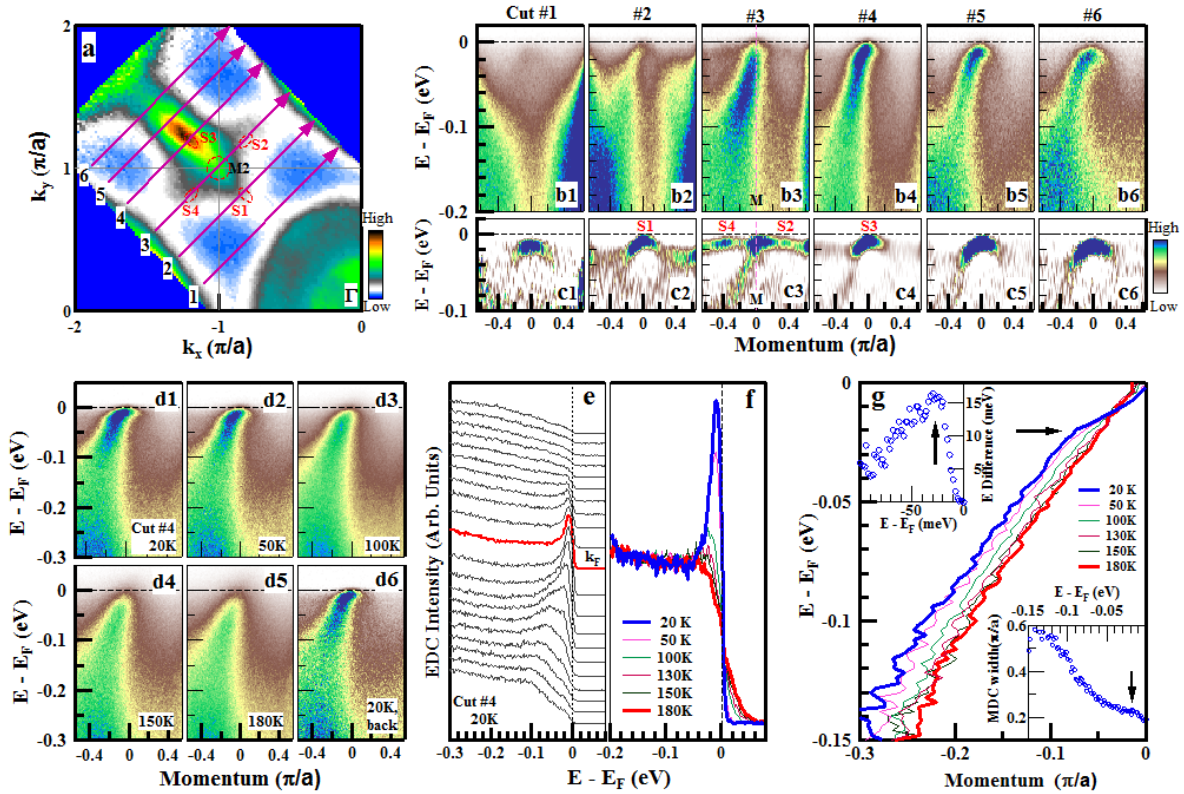


FIG. 4: Electronic structure of CeFeAsO near  $M2(-\pi, \pi)$ . (a). Spectral intensity as a function of  $k_x$  and  $k_y$  integrated over  $[-10 \text{ meV}, 10 \text{ meV}]$  energy window with respect to the Fermi level measured at 30 K. (b). Photoemission images at 6 typical momentum cuts with their location marked in Fig. 4a. (c). Corresponding second derivative images of Fig. 4b. (d). Photoemission images of the cut #4 measured at different temperatures, warming up from 20 K (d1) to 180 K (d5) and then cooling back to 20 K (d6). (e). EDCs of the cut #4 at 20 K corresponding to Fig. 4b4. (f). Temperature dependence of the EDCs at  $k_F$  of the cut #4. (g). Quantitative dispersions of the cut #4 at different temperatures extracted by fitting MDCs from photoemission images in Fig. 4d. A kink at  $\sim 25 \text{ meV}$  at low temperature is marked by the black arrow. The upper left inset shows the energy difference between the measured dispersion at 20 K and a straight line connecting two points on dispersion at  $E_F$  and  $-0.15 \text{ eV}$ . The corresponding MDC width at 20 K is shown in the lower right inset.

kink in dispersions occur at  $\sim 25 \text{ meV}$ , accompanied by a drop in the MDC width (bottom-right inset of Fig. 4g). The observations clearly indicate the existence of an energy scale at 25 meV which are reminiscent of the electron coupling with bosonic modes as seen in cuprate superconductors[25]. One possibility is that the kink is due to electron coupling to phonons. This scenario is consistent with the calculation of the Eliashberg function  $\alpha^2F(\omega)$  associated with electron-phonon coupling in LaFeAsO that exhibits an obvious peak near 25 meV[26]. Raman scattering also shows the existence of a particular  $B_{1g}$  phonon mode at  $\sim 25 \text{ meV}$  associated with the Fe vibrations[27]. We remark that this does not mean there are no other modes existing between 0 and 25 meV because the manifestation of multiple modes coupling may give rise to a similar kink at 25 meV[28]. Although electron-phonon coupling provides a likely origin of the kink, we cannot fully rule out other possibilities of electronic or magnetic origins. A hint of a  $\sim 25 \text{ meV}$  kink can also be seen near  $\Gamma$  in the  $\beta$  band (Fig. 2b), but not clear

in the  $\alpha$  band, suggesting its orbital-selective nature. As seen in the temperature dependence measurements (Fig. 4d and 4g), the kink develops below  $T_{MS}$  and gets enhanced at low temperatures, which indicates that the kink is closely related to the magnetic/structural transition. This is distinct from the kink reported in the superconducting  $(\text{Ba}_{0.6}\text{K}_{0.4})\text{Fe}_2\text{As}_2$  near the  $\Gamma$  point which is considered to be related to superconductivity[24, 29].

In summary, from our comprehensive ARPES measurements we find that CeFeAsO exhibits unusual electronic structure that deviates strongly from the band structure calculations. The electronic signature of the magnetic/structural transition shows up in the dramatic change of the quasiparticle scattering rate. We have identified for the first time a dispersion kink in this parent compound which is closely related to the magnetic/structural transition. These results provide a clear indication on the interplay between charge, spin and lattice in the FeAs-based parent compounds. These rich information also provide an opportunity to compare and con-

trast with other compounds in order to sort out universal features responsible for the FeAs-based superconductors. To better understand the unusual behaviors of these materials, further work needs to be done to well characterize the sample surface, particularly the surface doping or surface structure reconstruction.

We thank D.-H. Lee, T. Xiang, G.-M. Zhang, H. Zhai and Z. Y. Lu for helpful discussions. This work is supported by the NSFC, the MOST of China (973 project No: 2006CB601002, 2006CB921302, 2009CB929101) and CAS.

---

\* Corresponding author: XJZhou@aphy.iphy.ac.cn

- [1] Y. Kamihara et al., *J. Am. Chem. Soc.* **130**, 3296 (2008).
- [2] Z. A. Ren et al., *Chin. Phys. Lett.* **25**, 2215 (2008).
- [3] M. Rotter et al., *Phys. Rev. Lett.* **101**, 107006(2008).
- [4] F. C. Hsu et al., *Proc. Natl. Acad. Sci. USA* **105**, 14262 (2008).
- [5] X. C. Wang et al., *Solid State Commun.* **148**, 538(2008).
- [6] C. de la Cruz et al., *Nature (London)* **453**, 899(2008).
- [7] Q. Huang et al., *Phys. Rev. Lett.* **101**, 257003 (2008).
- [8] M. S. Torikachvili et al., *Phys. Rev. Lett.* **101**, 057006 (2008).
- [9] L. X. Yang et al., *Phys. Rev. Lett.* **102**, 107002 (2009).
- [10] C. Liu et al., *Phys. Rev. Lett.* **101**, 177005 (2008).
- [11] H. Y. Liu et al., *Phys. Rev. B* **78**, 184514 (2008).
- [12] V. B. Zabolotnyy et al., *Nature* **457**, 569 (2009).
- [13] D. Hsieh et al., arXiv:cond-mat/0812.2289.
- [14] G. D. Liu et al., *Phys. Rev. B* **80**, 134519 (2009).
- [15] M. Yi et al., *Phys. Rev. B* **80**, 174510 (2009).
- [16] T. Kondo et al., *Phys. Rev. Lett.* **101** (2008)147003.
- [17] D. H. Lu et al., *Physica C* **469**, 452 (2009).
- [18] G. D. Liu et al., *Rev. Sci. Instruments* **79**, 023105 (2008).
- [19] G. F. Chen et al., *Phys. Rev. Lett.* **100**, 247002 (2008).
- [20] D. J. Singh and M.-H. Du, *Phys. Rev. Lett.* **100**, 237003 (2008).
- [21] F. J. Ma et al., *Phys. Rev. B* **78**, 224517 (2008).
- [22] D. H. Lu et al., *Nature* **455**, 81 (2008).
- [23] L. Zhao et al., *Chin. Phys. Lett.* **25**, 4402(2008).
- [24] L. Wray et al., *Phys. Rev. B* **78**, 184508 (2008).
- [25] A. Lanzara et al., *Nature (London)* **412**, 510 (2001).
- [26] L. Boeri et al., *Phys. Rev. Lett.* **101**, 026403 (2008).
- [27] V. G. Hadjiev et al., *Phys. Rev. B* **77**, 220505(R) (2008).
- [28] X. J. Zhou et al., *Phys. Rev. Lett.* **95**, 117001 (2005).
- [29] P. Richard et al., *Phys. Rev. Lett.* **102**, 047003 (2009).